The electrical conductivity of the Andean crust in northern Chile and southern Bolivia as inferred from magnetotelluric measurements

G. Schwarz [1], V. Haak [1], E. Martínez [2] and J. Bannister [3]

[1] Institut für Geophysikalische Wissenschaften Freie Universität Berlin, Rheinbabenallee 49, D-100 Berlin 33
[2] Instituto de Investigaciones Físicas, UMSA Casilla 1464, La Paz, Bolivia
[3] Departamento de Geofísica, Universidad de Chile, Casilla 2777, Santiago, Chile

Abstract. The subducted Nasca plate produces anomalies of spectacular low electrical resistivity beneath the Andean knee. This is the result of two magnetotelluric field campaigns in 1982. The measurements were carried out on a profile from the Pacific coast to the Eastern Cordillera crossing northern Chile and southern Bolivia.

Several anomalies may be distinguished. The strongest anomaly has been detected beneath the Pre- and West-Cordillera, with resistivities around $0.5 \, \Omega m$ at depths greater than 5–10 km, strike direction roughly parallel to the main crest of the High-Cordillera. But also, the Altiplano is underlain – at a depth of 40–50 km – by very low-resistive material. In agreement with other geophysical and geological observations, we interpret these low resistivities as being due to the partially melted state. Further arguments identify the Pre-Cordillera anomaly, probably, with a plutonite which is still "alive", and the highly-conductive material 40 km beneath the Altiplano with the source of andesitic magma.

A crucial point in this study is the distinction between the E- and B-polarization of the apparent resistivities. We distinguished both polarizations by the direction of the induction arrows and by the lateral continuity of the apparent resistivity.

Key words: Electrical conductivity studies – Central Andes – Magnetotellurics – Crustal electrical resistivity anomaly – Partial melting – Temperature – Subduction processes – Plutonites – Andesitic volcanism – Separation of E- and B-polarization

Introduction

The Andes mountains began to rise when the Nasca plate began to submerge under western South America. This is a well known explanation of the Andes – part of any modern geoscience textbook.

What do we really know about motions and forces within the crust and upper mantle of the western South American mountain range? In fact, numerous geological investigations have been undertaken, and they have been used to reconstruct the motions and forces of the geological past. However, they do not allow a view to be formed on the present motions and forces. The present view on the ongo-

ing processes could be tackled by geophysical methods. In the past only a few methods have been tried in the Andes mountains. Seismology played the dominant role, by detecting Benioff zones down to 600 km depth (e.g. Ocola and Meyer, 1972; Luetgert and Meyer, 1981; James, 1971; Barazangi and Isacks, 1979; Stauder, 1973). Beside the abundant earthquake activity – superbly documented early in 1807 (Kleist, 1807) – the huge volcanos represent another most spectacular phenomenon of the Cordillera. Both Benioff zone and volcanic activities seem to be the witnesses of active plate tectonics. When Schmucker et al. (1964) reported the detection of one of the greatest anomalies of high electrical conductivity 20 km beneath the Andes in Peru, 400 km broad, the picture of the classical subduction zone became nearly perfect: magma rising from the Benioff plane to the upper crust, where it is stored in vast magma chambers – detected by high electrical conductivity – feeding the andesitic volcanos (Gough, 1973).

The big problem, namely the origin of the Andes mountains, seemed to be solved. However, a number of details were left unsolved; like the problem of the tremendous thickness of the Andean crust while no nappe tectonics are known, or the distribution of Cenozoic and Quaternary volcanic provinces, or the distribution of zones of earthquakes and of no earthquakes. Confining our discussion to the distribution of the electrical conductivity, it seemed questionable whether the famous Peruvian anomaly (Schmucker et al., 1964) continues to the south (Aldrich et al., 1975). In particular, it seemed questionable whether such a conductivity anomaly must be associated with an active submerging plate since the crust and upper mantle of Japan turned out to be very low conductive (Rikitake, 1969).

The problems might be even more complicated when fragments of continents, riding as plateaus on the oceanic plate, became involved in the subduction process (Nur and Avraham, 1982).

Considering the complexity of all the processes involved, the interdisciplinary effort of geoscientists is necessary to find the answers to the problem of the origin of the Andes mountains. This was the reason that the Free University and the Technical University of Berlin started an international project with scientists from Chile and Bolivia to investigate the crust and upper mantle of an east-west segment between 24° and 20° S, traversing the Andes from the Pacific ocean to the Brazilian shield.

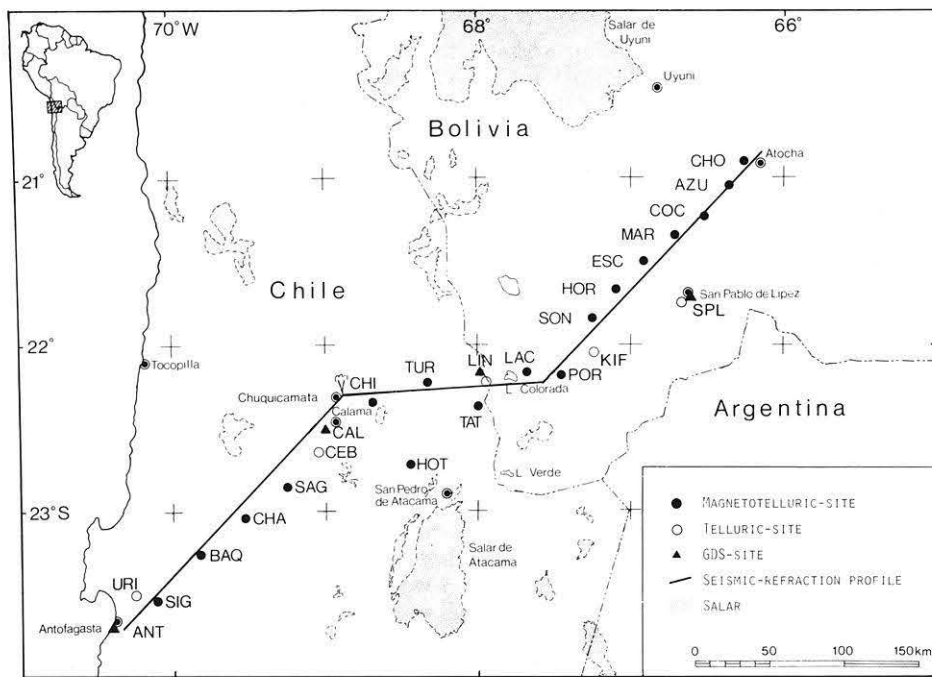Within this general research project, we measured the

Fig. 1. Map showing the locations of the magnetotelluric (*full circles*) and telluric (*open circles*) measuring sites in N-Chile and S-Bolivia, together with the locations of geomagnetic depth soundings (*full triangles*). At all sites, seismological measurements have been done as well. Also shown is the position of the seismic-refraction profile, on which shots from the Chuquicamata mine have been recorded (Wigger et al., 1983)

distribution of the electrical conductivity of the crust and upper mantle on a profile from the Pacific coast, over the Pre- and West-Cordillera, over the Altiplano to the Eastern Cordillera.

The electrical conductivity of rocks and minerals is related to temperature, composition and the state of the material. In this study we describe the method of how we determined the distribution of electrical conductivity, and we try to form a first interpretation in terms of temperature, composition and the state of the material. It will be left to another stage to consider all other results from geophysics, petrology, geology and others in order to find a more unique and more general answer.

Fieldwork

The magnetotelluric and geomagnetic depth soundings were made in spring and autumn, 1982. The profile which has been measured up to now starts at the Pacific coast in northern Chile, crosses (see Fig. 1) the Coastal Cordillera (ANT, SIG), the Pampa de Tamarugal (BAQ to CAL), the Pre- and W-Cordillera (CHI to LAC) and then goes into southern Bolivia, crossing the Altiplano (POR to CHO) and ends at the foothills of the E-Cordillera. The future plan of MT and GDS measurements within this project – foreseen to be carried out in autumn 1984 – will be the crossing of the E-Cordillera, the Sub-Andean zone, towards the lowland plains.

The actual profile covers a length of 550 km (Fig. 1). Observations were made at 13 sites in northern Chile and at 11 sites in southern Bolivia, the station spacing varying between 20 and 50 km. At all sites seismological measurements have also been carried out (Wigger et al., 1983), and seismic refraction measurements have been done on the profile shown in Fig. 1. For this study we have selected 13 out of the 24 sites for a first interpretation.

The instrumentation included 5-component magnetotelluric stations with fluxgate magnetometer, telluric device, digital recording system and paper chart recorder for direct control of measured data, for the period range from 15–10,000 s, and Askania mangetographs for the recording of long-period geomagnetic variations. The horizontal components of the electric field were measured by pairs of electrodes 100 m apart, using either Cu-$CuSO_4$ electrodes or an Ag-AgCl type (Filloux, 1973; Hempfling, 1977). At some places within the desert of Atacama in northern Chile impedances between the electrodes and the ground problematically reached critical values of more than 20 $M\Omega$. Resistivity mappings with a VLF-R instrument were not helpful at those places where the electrodes failed to operate. The resistivities of the uppermost subsoil normally varied between 100 and 2,000 Ωm. For better electrical contact between the electrodes and the ground, a mud of bentonite was used. All instruments were battery operated, being continuously recharged by solar generators. The recording time at one MT site varied between 2 and 3 weeks. The Askanias were operated at one place for at least 8 weeks.

The remote area under investigation and its harsh environment (extreme dust and wind and temperature changes of up to 40° C between day and night in the W-Cordillera and on the Altiplano) forced special precautions to be taken for the sake of the instruments – as well as for the persons engaged in the field work. All instruments were buried completely and isolated against direct sun.

Data analysis

All digital field data (electric and magnetic field) were plotted for visual control and to select the magnetically most active time intervals for further analysis, such that the period range 15–10,000 s is uniformly covered. From experiments in Tuscany/Italy (Schwarz, 1984), this subjective method turned out to be the most efficient method. Of a number of time intervals of about 4 days with enhanced magnetic activity, out of 2–3 weeks total recording time, a selection was chosen "by hand" in different combinations, to which the whole data analysis procedure – described later – was applied. The intention was to obtain

results which remain stable, though changing combinations of independent time intervals. This is the most important improvement, not even highly sophisticated mathematical methods can compensate failures in this state.

We considered results (i.e. apparent resistivities) as stable when different combinations of data sets did not change them significantly beyond their mean standard error. This procedure will exclude data which are not consistent with the majority of data. There may exist several reasons for inconsistency, but one, in particular is the potential drifts of electrodes.

After removing trends (linearly or as polynomials) and multiplying by a tapering window, the time intervals were transformed into the frequency domain. At this stage all instrumental filter characteristics are removed.

From the Fourier coefficients of the electric field $\mathbf{E}$ and magnetic field $\mathbf{B}$ the period-dependent transfer functions between electric and magnetic fields and between the vertical and horizontal magnetic field components are determined, following the linear equations

$$E_x = Z_{xx} B_x + Z_{xy} B_y,$$
$$E_y = Z_{yx} B_x + Z_{yy} B_y, \qquad \omega = \text{const} \quad (1)$$

and

$$B_z = Z_H B_x + Z_D B_y. \qquad (2)$$

The complex-valued coefficients Z_{xx}, Z_{xy}, Z_{xy}, Z_{yy}, and Z_H, Z_D are calculated by a least squares method.

The coordinate systems of minimum-maximum coherency

The calculation of the transfer functions yielded a strong polarization indicating a 2- or 3D structure. The question was whether we could distinguish transfer functions corresponding, at least approximately, to a 2D structure. This distinction (between a 2- and 3D structure) became crucial when, at some sites (CHI, TUR, TAT), the minor apparent resistivities with values below 1 Ωm turned out to be the E-polarization.

Such small resistivities could be an artefact produced by a 3D-distortion effect. Most workers in MT will rotate the coordinate system in order to reduce the diagonal terms Z_{xx} and Z_{yy} to zero. This method ultimately concentrates on the problem of which number really means zero. The answer distinguishes between 2- and 3D structure. We applied a slightly different method (Haak, 1972; 1978), which is based on the following philosophy.

In a strictly 2D anomaly, the magnetic component perpendicular to the strike corresponds to the E-polarization. Thus the electric field component is parallel to the strike. If we now consider a small local perturbation of the electrical conductivity, too small for an induction anomaly, superimposed on the strictly 2D anomaly, the electrical field will be distorted, i.e. the angle of polarization will be changed somewhat. The distortion is due to surface charges which do not affect the magnetic field.

This distortion means that the related components of the electric and magnetic field are not perpendicular to each other, as they are in 1D and 2D structures. Thus, in order to distinguish 2D and 3D structures we should determine this angle. Indeed, we can easily determine, at the first step, the mean polarization angle of the electric field which is either due to the polarization of the source field when no lateral conductivity structures exist, or due to such lateral conductivity structures. In order to find the direction of the corresponding magnetic field component we can proceed in the same way as we do to determine the magnetic induction arrow (Schmucker, 1970), just by replacing the vertical magnetic component by the electrical field component.

In practice, we applied the following algorithm (Haak, 1972). First the coordinate system is determined which yields minimum coherency between the orthogonal components of the electric field. This is the coordinate system of mean orientation of the elliptically polarized electric field, called the preference direction. Second, the coordinate system of the magnetic field is rotated until the coherency between the electric and magnetic fields reaches a maximum.

What can we expect, and infer, from our method of coordinate rotation?

1. The dimension of the lateral conductivity structure
a) 1D: The coordinate systems of the electric and magnetic field are different by 90°, the absolute angle of rotation differs from period to period, dependent only on the distribution of the polarization angles of the inducing magnetic field.
b) 2D: Again, electric and magnetic field coordinate systems are 90° different; but the angle of rotation is constant and independent of period. One orientation of the coordinate system corresponds to the E-polarization, the other coordinate system to the B-polarization. The distinction of both polarizations is crucial and will be discussed in a subsequent section.
c) 3D: The coordinate systems of electric and magnetic fields are not orthogonal to each other anymore, independent of the period. For interpretation, we may possibly approximate it by a locally varying 2D structure, but it would be better to apply more sophisticated separation methods, as Larsen (1975) has proposed.

2. The direction of maximum coherency will display the direction of 2D induction anomalies much more correctly than induction arrows, if there exist more than one anomaly. Induction arrows between two anomalies may cancel each other incompletely, thus pointing to some irrelevant direction. This cannot happen to the maximum coherent coordinate system because the electric fields do not cancel each other.

Results of data analysis

A result, representative of most of the sites, is displayed in Fig. 2. It shows the apparent resistivities $\rho_{a,\text{max}}$ and $\rho_{a,\text{min}}$, the phases φ_{max}, φ_{min}, the preference direction (mean polarization angle) of the electric field (AZIME) and the direction of the most coherent magnetic field (AZIMB).

Site TAT (El Tatio) represents the sites where the coordinate systems are constant and independent of period between 25 and 4,000 s. The maximum and minimum resistivity curves are separated by an order of magnitude, thus urging a clear identification of E- and B-polarization. A most important observation is the stable orthogonality between electric and magnetic coordinate systems, which clearly points to a 2D conductivity anomaly.

Site ESC (Mina Escala) represents the case where the coordinate systems rotate with increasing period, but remain constantly separated by 90°. This "behaviour" points to a weak 2D- or approximate 1D-conductivity structure
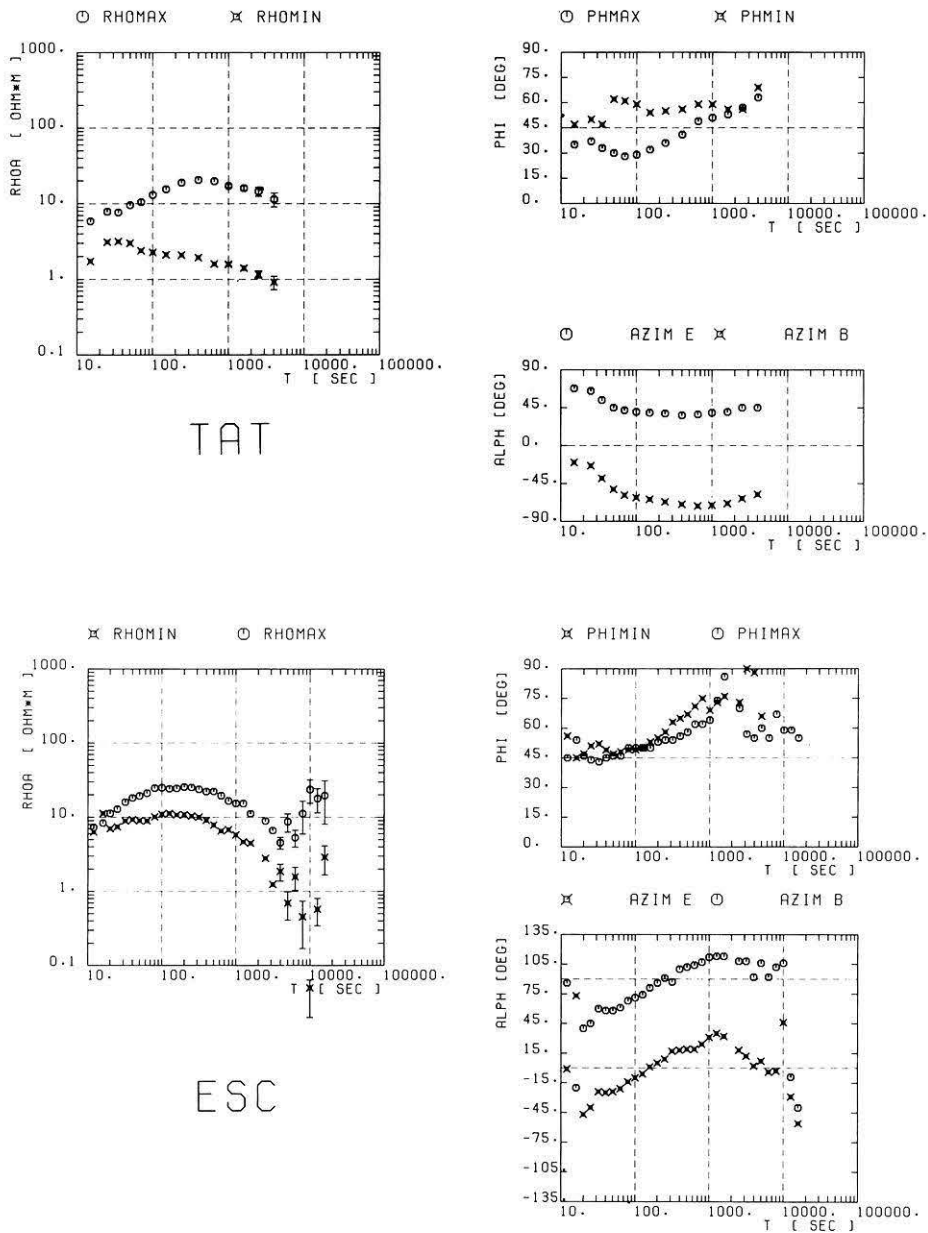
Fig. 2. Apparent resistivities ρ_a as a function of period T for the sites TAT (in the W-Cordillera) and ESC (on the Altiplano), together with phase differences φ between the electric and magnetic field and rotation angles of the electric (Azim E) and magnetic field (Azim B). Error bars are only given if larger than symbols

where the changing angles of rotation are determined by the changing angles of polarization of the magnetic source field.

The identification of E- and B-polarization

At some sites the maximum and minimum resistivity curves are separated by orders of magnitude. Since the coordinate systems of the electric and magnetic field turned out to be orthogonal to each other, we may infer the 2D character of the conductivity structure. Therefore, one of the apparent resistivities should correspond to the E-polarization, the other one to the B-polarization. We applied two different methods to accomplish the identification.

Interpretation of induction arrows (Schmucker-Wiese). The transfer functions of the vertical magnetic field can be displayed in the form of induction arrows (Schmucker, 1970)

$$
\begin{aligned}
0°\text{-arrow} \quad a_{Re} &= Re(Z_H) \cdot e_x + Re\,(Z_D) \cdot e_y \\
90°\text{-arrow} \quad a_{Im} &= Im(Z_H) \cdot e_x + Im\,(Z_D) \cdot e_y,
\end{aligned} \tag{4}
$$

with e_x, e_y as unit vectors in N and E directions.

In a clear, simple 2D-conductivity structure all induction vectors are perpendicular to the direction of the strike and point away from the well-conducting anomaly. The direction of the E-polarization will then be the direction perpendicular to the induction arrow. It is, therefore, easy to separate E- and B-polarization in a simple 2D structure, even if the structure is hidden, just by looking at the induction vectors.

However, in a more complex anomaly the identification may become impossible. Consider two 2D anomalies of different strike direction, which are near each other compared to the relevant skin depth. In this case, we may expect the superposition of magnetic fields induced in each anomaly (and also of mutual induction). It may easily turn out
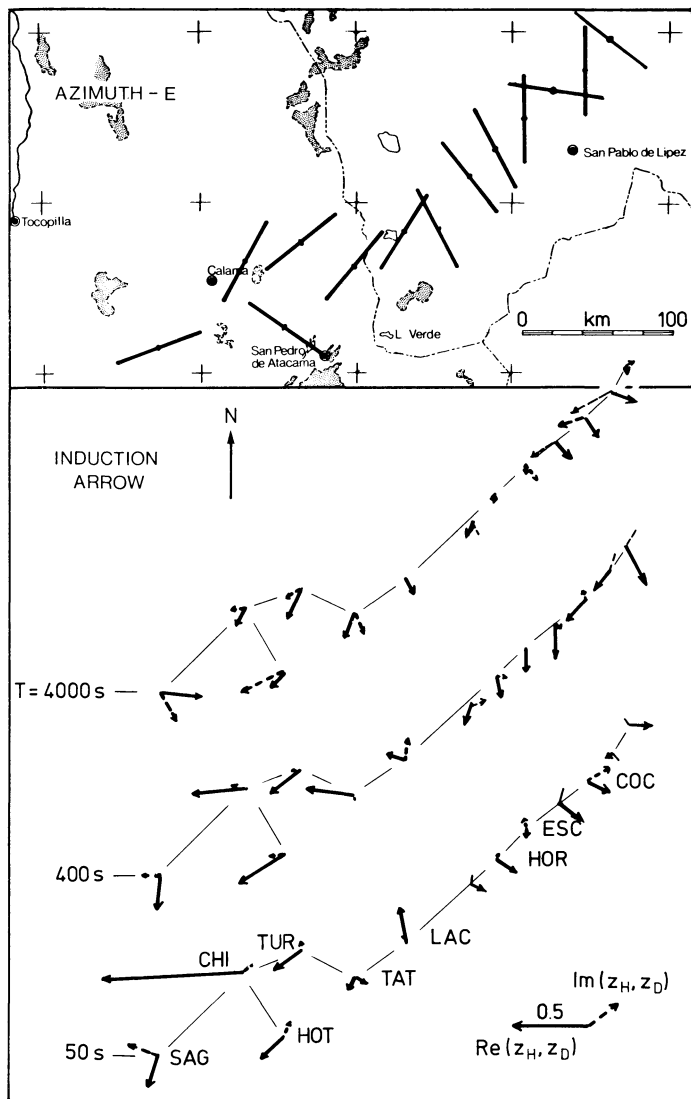
Fig. 3. *Upper section* represents preference directions of the induced electrical field on the profile from the Pre-Cordillera to the border of the E-Cordillera. The *bars* (in unit length) show the mean direction of *E*-field for periods from 50 to 1,000 s. The *lower section* gives the induction arrows, derived from the recordings of the earth magnetic field (*T*: 50, 400, 1,000 s). The *arrows* are pointing away from the induction anomaly!

that the resulting induction arrow has no more relevance to the strike direction of the anomaly.

A) The situation in northern Chile.

Looking at the induction arrows in Fig. 3, in particular in northern Chile, the arrows, in general, point towards the Pacific Ocean, away from a conductivity anomaly somewhere under the Pre- and W-Cordillera. Near Calama – between CAL and SAG – the western border of this extremely good conductor can be suggested. The induction arrows at SAG, very probably, are already influenced by the ocean.

The most important feature of the induction arrows in N-Chile is their direction, which is parallel to the preference direction of the electric field. This is the direction of the $\rho_{a,\,max}$ component. It follows that the extraordinarily small $\rho_{a,\,min}$ curves (e.g. at site TAT, Fig. 2) represent the *E*-polarization.

B) The situation in southern Bolivia.

In the centre of the Altiplano, the preference directions of the electric field are parallel to the strike of this sedimen-

tary basin, and should, therefore, indicate the direction of the *E*-polarization. The induction arrows are vanishingly small in the centre. Further towards the eastern border the arrows point towards SE, probably indicating the border of the huge sedimentary basin of the Altiplano nearby.

The continuity of the E-polarized apparent resistivity. The continuity of the electric field component parallel to elongated conductivity structures offers another possibility of identifying the *E*-polarization. It is indeed an alternative method, compared with the induction vector method. Consider again the sites between two 2D anomalies of slightly different strike. The induction arrows originating from both anomalies cancel each other incompletely, leaving a residual arrow which has no relation to both anomalies. Alternatively, the electric field components parallel to the strike direction (*E*-polarization) are in the same direction, and laterally continuous. The component of the electric field perpendicular to the strike (*B*-polarization) "jumps" discontinuously from site to site. We could proceed now by starting to rotate the coordinate systems again. But here we want to check the minimum-maximum coordinate systems and whether the results obtained already agree with the continuity and discontinuity rules. Proof would be the continuity
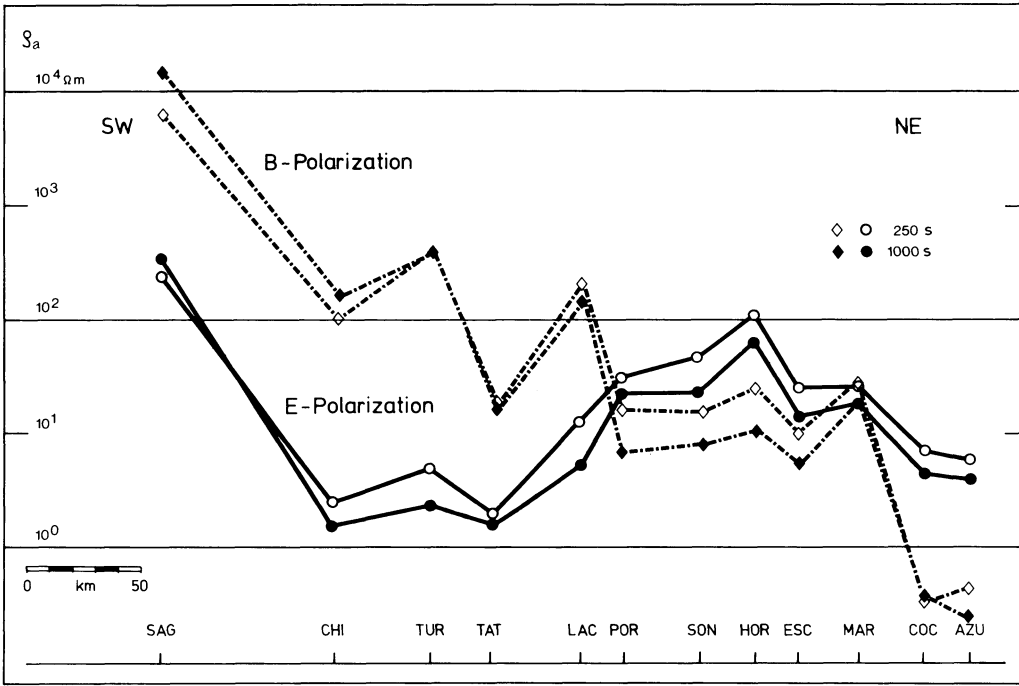
Fig. 4. Variation of *E*-polarization (*full lines*) and *B*-polarization (*dashed lines*) apparent resistivities ρ_a (in Ωm) along the profile from site SAG to site AZU for periods of 250 and 1,000 s. Note that the *E*-polarization curves are the continuous curves, as we should expect!
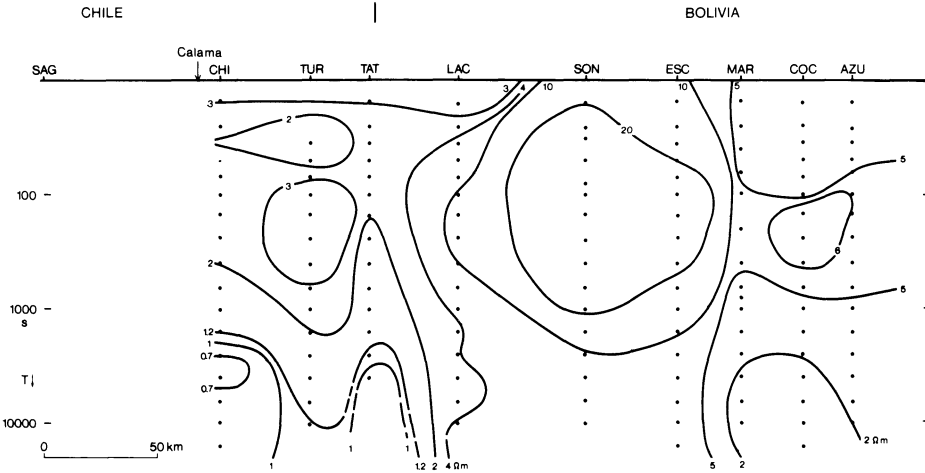

Fig. 5. Pseudo-section of *E*-polarization apparent resistivity ρ_a (in Ωm) for periods from 10 to 10,000 s along the profile from the Pre- to the E-Cordillera

of the *E*-polarization, as opposed to the discontinuity of the *B*-polarization. This is demonstrated in Fig. 4. The variation of apparent resistivities for *E*- and *B*-polarization is given for two periods. The *E*-polarization curve along the profile is a continuous one, whereas the *B*-polarization curve is "jumping up and down". Only on the Altiplano are both ρ_a-curves almost continuous and equal, displaying isotropic conductivity structures beneath the Altiplano.

If the 2D structure (responsible for the splitting into two different modes) is restricted to the upper few kilometres of the crust, whilst the deeper conductivity structure is dependent on depth only, the $\rho_{a,\text{E-pol}}$ may be interpreted by a 1D-model. In Fig. 5 all apparent resistivities along the profile, corresponding to the *E*-polarization, are combined in a pseudo-section. The vertical axis gives the downward increasing period *T*. Increasing period means, in any

case, an increasing penetration depth, thus the vertical axis displays a kind of depth-scale, too. Roughly, two areas of different electrical conductivity structure can be distinguished within the section: (a) the Pre- and W-Cordillera with apparent resistivities of clearly less than 1 Ωm at 1,000 s; (b) the Altiplano with higher apparent resistivities in the medium period range.

Model search

First approximation models

The pseudo-section in the last section is a useful way to present data but not to present a model, because the pseudo-depth scale "period" is much too distorted. A much more useful presentation is $\rho^*(z^*)$ (Schmucker, 1971) which
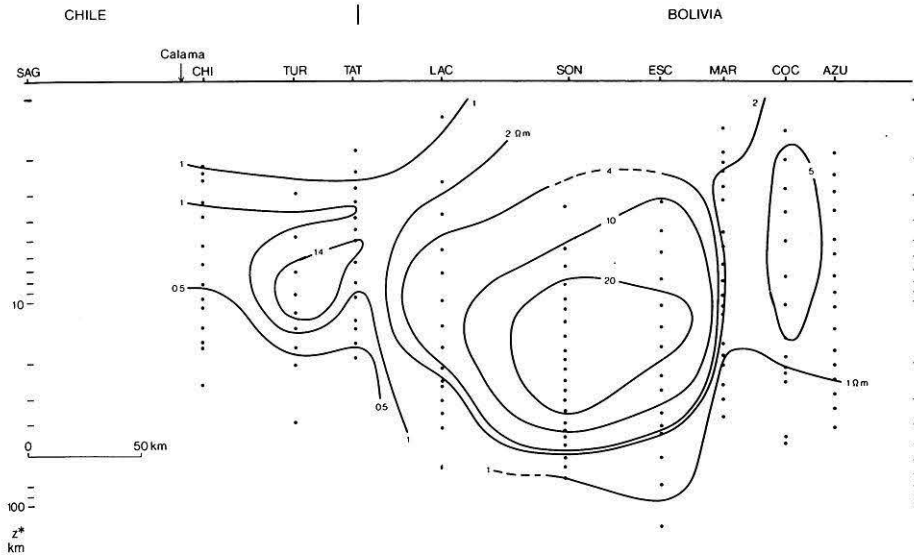
Fig. 6. Section with resistivity ρ^* versus corresponding penetration depth z^*, calculated from apparent resistivity ρ_a and phase φ for E-polarization case. The resistivity distribution with depth becomes much clearer than in Fig. 5: the upper crust at depths greater than 10 km of the Pre- and W-Cordillera is characterized by extreme low resistivities of 0.5 Ωm and less, whereas the crust of the Altiplano at this depth range has electrical resistivities of more than 20 Ωm
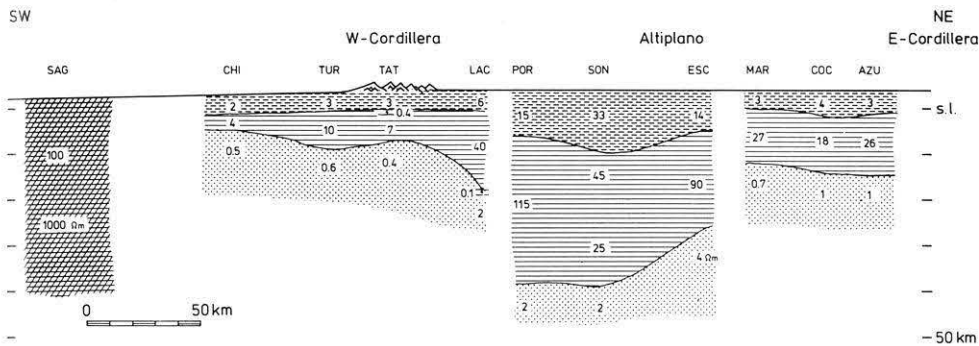

Fig. 7. One-dimensional models of resistivity distribution along the profile from SW towards NE, calculated with Schmucker's (1974) ψ-algorithm. Shading of layers might only be a first attempt at a complete resistivity model, but one can obviously distinguish three well-conducting layers in the crust: a highly conducting upper crust beneath the Pre- and W-Cordillera, a good conductor in the lower crust beneath the Altiplano, and a highly conducting upper crust at the border of the E-Cordillera

acts as both a presentation of data and as a first, undistorted but still very tentative view of the model, see Fig. 6. We may distinguish at least two main parts, namely the western part including the Pre- and the W-Cordillera and the eastern part including the Altiplano and the border of the E-Cordillera. The western part, west of Calama, displays a transition from high-resistivity structure to low-resistivity, with extreme low-resistivity values at a depth of about 10 km. The eastern part, the Altiplano area, consists of three stories, namely a low-resistivity layer at the top, a high-resistive central story underlain by low-resistive material.

The low-resistive western part and the eastern part show smooth lateral changes of resistivity. The obvious strong polarization of the electric field and apparent resistivities should be caused, therefore, by lateral resistivity changes in the uppermost kilometre. The resistivity of the uppermost layer has not been resolved by the shortest periods, which can also be seen in Fig. 6 from the smallest z^* values. We, therefore, conclude that we may proceed with the model search by 1-dimensional modelling at each site separately. This will be done with the help of the ψ-algorithm of Schmucker (1974).

1D-model inversion

A more distinct resistivity-depth function can be obtained by the ψ-algorithm (Schmucker, 1974) using both apparent resistivities and phase differences. This method does not give any information about the actual number of layers present, except the minimum number necessary to explain the measured resistivities and phase differences. It is in this sense that the 1D-layer models in Fig. 7 are to be understood. The question is, which of the model parameters (thickness d_i and resistivities ρ_i) are well determined and which are not? It is well known (e.g. Keller and Furgerson, 1977; Edwards et al., 1981) that the depth to the upper surface of a low-resistive layer is a well-determined parameter. This holds here for the low-resistive layer beneath the Pre- and W-Cordillera. Another well-determined parameter is the total conductance d_1/ρ_1 of the uppermost layer of the Altiplano. Only separate measurements of ρ_1 can resolve the depth d_1. A less resolved parameter in each model is the resistivity of the central high-resistive layer.

Since all the 1D models obtained turned out to be of the same type, a maximum type, we connected the interfaces of the different models, except at the transition from the

West-Cordillera to the Altiplano and at the transition from the Altiplano to the E-Cordillera (Fig. 7). We thought these two hiatus necessary, since Fig. 6 suggested such a division. It is difficult to decide whether this division is meaningful just by induction studies, since the resolution is too small. The petrological discussion in the next section will be – at least – easier. A final decision can only be made by incorporating other geophysical results (Giese et al., in preparation).

The most important results in Fig. 7 are the highly conducting "layer" ($\rho \approx 0.5\ \Omega m$) 10 km beneath the Pre- and W-Cordillera and the well-conducting "layer" 40 km beneath the Altiplano. We will try to find a plausible petrological answer to these two geophysical questions. Finally, it must be mentioned that we did not find the lower surface of the high-conducting layer, since the analysed periods were too small.

A petrological model

A number of petrological models of subduction zones are known which are based on geological, geophysical and laboratory data (e.g. Ringwood, 1975). The question here is, which new details can be inferred from the electrical conductivity structures presented in the preceding sections and which details contribute to known petrological models? An important step is to transform the conductivity structures into petrological parameters. Rather little is known up to now about the deep conductivity in the currently most active subduction zones. The investigations of the Japanese conductivity anomaly (Rikitake, 1975) and of the Peruvian anomaly (Schmucker et al., 1966) are the most famous. They will be considered at the end of this section.

The electrical conductivity is related to temperature, composition and state of material. In general, it should be quite impossible to distinguish between these possible causes of low and high resistivities. However, considering those copious amounts of material of such extreme resistivities as low as 0.5 Ωm at depths of about 5–10 km beneath the Pre- and W-Cordillera and at a depth of about 40 km beneath the Altiplano (cf. Fig. 7), only a very few candidates will remain for interpretation.

It seems convenient to divide the whole profile into several "units" which, very probably, deserve different explanations. Four parts will be distinguished: (I) Pacific Coast-CAL: high crustal resistivities; (II) CAL-LAC: extremely low resistivities (0.5 Ωm) below 5–10 km depth; (III) Altiplano: low resistivity in the upper 10 km, high resistivity in the middle crust and unusual low-resistivity values at a depth of 40 km; (IV) at the eastern side of the Altiplano the low-resistive layers rise from 40 km to about 20 km depth.

We want to pick out only two most extraordinary items of all these phenomena: the Pre-Cordillera anomaly (II) and the Altiplano (III) anomaly.

Candidates

Without any additional knowledge, some solid state compositions, e.g. abundant graphite, could very well explain the low resistivities in anomaly II and III. However, observations like the extreme absorption of seismic energy (Molnar and Oliver, 1969) in northern Chile indicate a fluid state composition. We may exclude abundant free water since

it may easily rise to the earth's surface due to its low density and also low viscosity (fluids rising in dynamical moving cracks). The only serious candidates for an abundant, low-resistive material remain partially molten rocks. The existence of melts is reasonable in these areas, in particular, from the point of view of the known petrology of subduction zones. As will be discussed later, the existence of melts may also be correlated with a number of other non-electric phenomena.

Amount of melt

The electrical resistivity of all types of melt, independent of their SiO_2 content, is very low ($\approx 0.1\ \Omega m$) compared with the resistivity of the solid, crystalline counterpart ($\approx 1{,}000\ \Omega m$). The resistivity of both states, however, is dependent on temperature (see Haak, 1982 for a review). Since rocks do not melt at one instance in time but do so gradually from their solidus temperature towards their liquidus temperature, we have to deal in most cases with partially melted rocks. During the last 10 years considerable effort was made to correlate the electrical resistivity of fluid-filled, e.g. partially melted, rocks with the percentage of the fluid (Waff, 1974; Shankland and Waff, 1977; Chelidze, 1978; Honkura, 1975; Hermance, 1979). The problem was the unknown, or partially known, geometry of the fluid distribution within the solid matrix. Most authors however agreed that two extreme models of fluid distribution determine the lower and upper bound of the electrical resistivity of a partially fluid-filled rock, which coincided with the extreme models of Maxwell (1892): (1) isolated, highly resistive spheres in a low-resistive, interconnected fluid on the one side, and (2) isolated, low-resistive "droplets" in a high-resistive rock matrix on the other side.

Now using the "upper bound curve" of model I in order to calculate the lowermost possible percentage of melt, we use the formula

$$V_m = 3\sigma / (2\,\sigma_m - \sigma),$$

which is the inversion of Maxwell's equation, by setting

$\sigma_0 = 0$ (conductivity of solid matrix),

$\sigma\ \ =$ measured, effective conductivity,

$\sigma_m =$ conductivity of melt.

Let

$\sigma_m = 10$ S/m

$\sigma\ = 2$ S/m (conductivity measured at 10 km depth beneath the Pre- and W-Cordillera),

then $V_m = 33\%$.

For

$\sigma = 0.5$ S/m (40 km beneath the Altiplano), $V_m = 8\%$.

Stability of melt

The problem posed here is not the existence of melt at all, but the apparent contradiction between these copious amounts of melt beneath the Pre- and Western-Cordillera and the sparse volcanism at the earth's surface: no volcanism exists in the Pre-Cordillera! We may consider two types of stabilization of melt: (1) The density of melt is higher than the density of the material around and above

it. (2) The viscosity of the melt increases considerably by many orders of magnitude when the effective pressure drops, i.e. when melt tries to rise to the earth's surface. Such behaviour is known for SiO_2-rich and water-abundant melts (Kushiro et al., 1976). These melts tend to polymerize when pressure is released, leading to highly viscous melts in the upper crust. Indeed, we may expect such acid melts in the upper crust in this area since plutonites of acid composition are known from Jurassic to Tertiary time, with an increasing intrusive age from W to E (Breitkreuz and Berg, 1983).

If we linearly extrapolate their age-distance relationship of plutonites and shift it, parallel, from latitude 26° S to about 22° S, then we might indeed infer that the low-resistive anomaly at 5–10 km depth, over a distance of nearly 100 km, is the present "plutonite".

The interpretation of the low resistivity 40 km beneath the Altiplano is much more a matter of speculation. It seems difficult to find any other explanation than that of partial melt (10% by volume). Indeed, there exist petrological models which predict such melted regions at these depths (e.g. Wyllie, 1981).

Correlations

We argue that the low resistivities beneath the Pre- and W-Cordillera indicate acid, grano-dioritic or granitic melts; the low resistivity beneath the Altiplano indicates basic melts. Which other arguments can support this hypothesis? Following the laboratory measurements on granites at various water pressures by Lebedev and Khitarov (1964), a temperature of only 700° C suffices to explain 0.5 Ωm. Such a temperature would not initiate any volcanic processes. However, heat flow measurements are not yet known for this area. On the crest of the Western-Cordillera, the geothermal anomaly of El Tatio reveals pure SiO_2 exhalation (Zeil, 1959). No sulphuric exhalations are known, as in most geothermal anomalies, pointing to a differentiated, acid composition in the upper crust.

A source of water

It is obvious that such low-resistive melts as detected in the Pre- and W-Cordillera are only possible when an abundant source of water exists in the lower crust or upper mantle. In areas of ascending mantle material as, e.g. in Iceland (Beblo and Björnsson, 1978; 1980), we do not need such a source of water, since the resistivities with values of about 10 Ωm are distinctly higher.

Therefore, the water necessary to create the vast, acidic plutonite does not originate from the original upper mantle material, but must originate from the subducted material. Indeed, the Pre-Cordillera anomaly is situated exactly 100 km above the Benioff zone, i.e. where a pressure regime of around 30 kbar transforms amphibolites into free water and eclogite (Ringwood, 1975; Wyllie, 1981).

The production of melt

The free water rises from a depth of about 100 km, e.g. embedded in cracks, to the earth's surface. With this transport, a certain amount of heat is also conveyed to the upper layers. When this water invades the crustal rocks through the Moho, it depresses the solidus temperature to values of about 600°–700° C. Since such temperatures may indeed exist by the heat transported from the upper mantle, the rocks begin to melt, convect and differentiate so that, finally, acid melt exists in the upper crust, superposed on less acid rocks.

A petrological model?

We suggest that our measurements of the electrical conductivity of the Andean crust reveal two phenomena. First, a still partially melted plutonite beneath the Pre- and W-Cordillera and secondly, a source of magma beneath the Altiplano.

The question is, whether this petrological model is normal and typical of all subduction zones? We may transform this question back to the question of whether these conductivity distributions are also detected in other subduction zones?

The general answer is: no. In Japan (Rikitake, 1969; 1975) the situation is just the opposite: the upper mantle beneath Japan is highly resistive.

However, one might correlate our conductivity anomaly with the Peruvian anomaly (Schmucker et al., 1964), at least genetically. If we need the subducted oceanic lithosphere as the source of free water at about 100 km depth, then the angle of subduction should be less than beneath our profile in order to shift the anomaly further to the east than the Pre-Cordillera anomaly. The most recent interpretation of the Peruvian anomaly (Schmucker, 1973) yielded 20 km as the depth of the upper surface of the anomaly and 10 Ωm as its resistivity. However, considering the long period of 1 h used and the reduced resolution of the applied method (Edwards et al., 1981), these values may also be much less and thus comparable to our values of the Pre-Cordilleran anomaly.

To the south of our profiles the pattern of conductivity anomalies seem to get more complicated (Febrer et al., 1981). It is clear that we cannot just draw contour lines of equal electrical conductivities parallel to the strike of the trench at the west coast of South America. Probably, the distribution of high electrical conductivity depends strongly on the dipping angle of the oceanic plate, the degree of hydration and dehydration, on the subduction speed, on possibly "consumed" terrains (Nur and Avraham, 1982) and many more "parameters". In each case the electrical conductivity is a parameter which is most sensitive to processes which are related to the subduction of the oceanic plate.

References

Aldrich, T., Bannister, J., del Pozo, S., Salgueiro, R., Beach, L.: Electrical conductivity studies in South America-Chile-Bolivia. Carnegie Inst. Wash. Yearb. 292–293, 1975

Barazangi, M., Isacks, B.L.: Subduction of the Nazca plate beneath Peru: evidence from spatial distribution of earthquakes. Geophys. J.R. Astron. Soc. 57, 537–555, 1979

Beblo, M., Björnsson, A.: Magnetotelluric investigation of the lower crust and upper mantle beneath Iceland. J. Geophys. 45, 1–16, 1978

Beblo, M., Björnsson, A.: A model of electrical resistivity beneath NE-Iceland, correlation with temperature. J. Geophys. 47, 184–190, 1980

Breitkreuz, Ch., Berg, K.: Magmatite in der Küstenkordillere südöstlich von Chañaral/Nordchile. Zbl. Geol. Paläont. Teil 1, H. 3/4, 387–401, 1983

Chelidze, T.L.: Structure-sensitive physical properties of partially melted rocks. Phys. Earth Planet. Inter. 17, 41–46, 1978

Edwards, R.N., Bailey, R.C., Garland, G.D.: Conductivity anomalies: lower crust or asthenosphere? Phys. Earth Planet. Inter. 25, 263–272, 1981

Febrer, J.M., Gasco, J.C., Pomposiello, C., Mamami, M., Baldis, B., Fournier, H.C.: Magnetotelluric measurements defining a continental mantle plume in a zone of the Andean belt southeast of the Altiplano in Argentine. Paper presented at 4th IAGA Soc. Ass., Edinburgh, 1981

Filloux, J.H.: Techniques and instrumentation for study of natural electromagnetic induction at sea. Phys. Earth Planet. Inter. 7, 323–338, 1973

Gough, D.I.: The geophysical significance of geomagnetic variation anomalies. Phys. Earth Planet. Inter. 7, 379–388, 1973

Haak, V.: Bestimmung der Übertragungsfunktionen in Gebieten mit lateraler Änderung der elektrischen Leitfähigkeit. Z. Geophys. 38, 85–102, 1972

Haak, V.: Interpretationsverfahren für die Magnetotellurik unter besonderer Berücksichtigung lateral variierender elektrischer Leitfähigkeit im Erdinnern und eines räumlich inhomogen induzierenden Magnetfeldes. Bayer. Akad. Wiss. Math.-Nat. Klasse München 158, 1978

Haak, V.: Elektrische Leitfähigkeit von Mineralen und Gesteinen bei hohen Drücken und Temperaturen. In: Landolt-Börnstein, Bd. V/1b, Physikalische Eigenschaften der Gesteine, G. Angenheister, ed.: pp 291–307. Berlin: Springer, 1982

Hempfling, R.: Beobachtung und Auswertung tagesperiodischer Variationen des erdelektronischen Feldes in der Umgebung von Göttingen. Diss. Math.-Nat. Fak. Univ. Göttingen, 1977

Hermance, J.F.: The electrical conductivity of materials containing partial melt: a simple model from Archie's law. Geophys. Res. Lett. 6, 613–616, 1979

Honkura, Y.: Partial melting and the electrical conductivity anomalies beneath the Japan and Philippine Seas. Phys. Earth Planet. Inter. 10, 128–134, 1975

James, D.E.: Andean crustal structure. Carn. Inst. Wash. Yearb. 69, 447–460, 1971

Keller, G.V., Furgerson, T.B.: Determining the resistivity of resistant layer in the crust. In: The Earth's crust, J.G. Heacock, ed.: pp 440–469, Geophys. Monogr. 20, AGU, Washington: 1977

Kleist, H.v.: Jeronimo and Josephe. Eine Szene aus dem Erdbeben zu Chili, vom Jahr 1647. Morgenblatt für gebildete Stände. 10–17. Sept. 1807

Kushiro, J., Goder, H.S. Jr., Mysen, B.O.: Viscosities of basalt and andesite melts at high pressures. J. Geophys. Res. 81, 6351–6356, 1976

Larsen, J.C.: Low frequency (0.1–6.0 cpd) electromagnetic study

of deep mantle conductivity beneath the Hawaiian Islands. Geophys. J.R. Astron. Soc. 43, 14–56, 1975

Lebedev, E.B., Khitarov, N.I.: Dependence of the beginning of melting of granite and the electrical conductivity of its melt on high water vapour pressure. Geochem. Int. 1, 193–197, 1964

Luetgert, J.H., Meyer, R.P.: Crustal structure of coastal Peru, 12° S to 16.2° S latitude. Paper presented at 21st IUGG General Assembly, London, Canada, 1981

Maxwell, J.C.: A treatise on electricity and magnetism. Oxford: Clarendon, 1892

Molnar, P., Oliver, J.: Lateral variations of attenuation in the upper mantle and discontinuities in the lithosphere. J. Geophys. Res. 74, 2648–2682, 1969

Nur, A., Avraham, Z.B.: Oceanic plateaus, the fragmentation of continents, and mountain building. J. Geophys. Res. 87, 3644–3661, 1982

Ocola, L.C., Meyer, R.P.: Crustal low-velocity zones under the Peru-Bolivia Altiplano. Geophys. J.R. Astron. Soc. 30, 199–209, 1972

Rikitake, T.: The undulation of an electrically conductive layer beneath the islands of Japan. Tectonophysics 1, 257–264, 1969

Rikitake, T.: A model of geoelectric structure beneath Japan. J. Geomagn. Geoelectr. 26, 233–244, 1975

Ringwood, A.E.: Composition and petrology of the Earth's mantle. New York: McGraw Hill 1975

Schmucker, U., Hartmann, O., Giesecke, A.A. Jr., Casaverde, M., Forbush, S.E.: Electrical conductivity anomaly in the Earth's crust in Peru. Carn. Inst. Washington Yearbook 63, 354–362, 1964

Schmucker, U., Forbush, S.E., Hartmann, O., Giesecke, A.A., Casaverde, M., Castillo, J., Salgueiro, R., del Pozo, S.: Electrical conductivity anomaly under the Andes. Carnegie Inst. Wash. Yearb. 65, 11–28, 1966

Schmucker, U.: Anomalies of geomagnetic variations in the southwestern United States. Bull. Scripps Inst. Ocean. Univ. Calif. 13, 1970

Schmucker, U.: Neue Rechenmethoden zur Tiefensondierung mit langperiodischen Variationen. In: Prot. Koll. Erdmagn. Tiefensond., P. Weidelt, ed.: pp 1–39, Göttingen: 1971

Schmucker, U. Regional induction studies: a review of methods and results. Phys. Earth Planet. Inter. 7, 365–378, 1973

Schmucker, U.: Erdmagnetische Tiefensondierung mit langperiodischen Variationen. In: Prot. Koll. Erdmagn. Tiefensond., A. Berktold, ed.: pp 313–342, München: 1974

Schwarz, G.: Die elektrische Leitfähigkeit in der Toskana und ein daraus abgeleitetes geothermisches Modell – insbesondere für die Anomalie von Travale. Berliner Geowiss. Abh. (B) 8, 1984

Shankland, T.J., Waff, H.S.: Partial melting and electrical conductivity anomalies in the upper mantle. J. Geophys. Res. 82, 5409–5417, 1977

Stauder, W.: Mechanism and spatial distribution of Chilean earthquakes with relation to subduction of the oceanic plate. J. Geophys. Res. 78, 5033–5061, 1973

Waff, H.S.: Theoretical considerations of electrical conductivity in a partial molten mantle and implications for geothermometry. J. Geophys. Res. 79, 4003–4010, 1974

Wigger, P., Giese, P., Kausel, E., Ricaldi, E.: Seismologische und refraktionsseismische Untersuchungen in den Zentral-Anden auf einer Traverse von der pazifischen Küste bis zur Ostkordillere. Contributed paper at 43rd DGG-meeting Aachen, 1983

Wyllie, W.J.: Plate tectonics and magma genesis. Geol. Rundsch. 70, 128–153, 1981

Zeil, W.: Das Fumarolen- und Geysir-Feld westlich der Vulkangruppe des Tatio (Provinz Antofagasta, Chile). Bayer. Akad. Wiss. Math.-Nat. Klasse München 96, 1959